



# Fluorescent Carbon Quantum Dots with Fe(III/II) Ions as Bridge for the Detection of Ascorbic Acid and H<sub>2</sub>O<sub>2</sub>

Kuan Luo<sup>1</sup> · Xinyu Jiang<sup>1,2</sup>

Received: 15 March 2019 / Accepted: 28 May 2019 / Published online: 5 June 2019  
© Springer Science+Business Media, LLC, part of Springer Nature 2019

## Abstract

Nitrogen-sulfur co-doped carbon quantum dots (N, S-CQDs) with good photoluminescence properties were prepared by hydrothermal method using citric acid (CA) and methionine (Met) as precursors. Co-doping with N and S facilitates the electron transfer rate and coordination interaction between N,S-CQDs and Fe(III) ions which acts as a quencher of fluorescence. Based on a simple redox principle, a highly sensitive and selective method for the detection of ascorbic acid (AA) and H<sub>2</sub>O<sub>2</sub> was successfully developed. The calibration curves obtained are linear for the current versus AA and H<sub>2</sub>O<sub>2</sub> concentration over the range 50–500 μM and 10–140 μM, respectively. And the detection limits for AA and H<sub>2</sub>O<sub>2</sub> are 4.2 μM and 1.9 μM, respectively. The quantitative analysis of AA and H<sub>2</sub>O<sub>2</sub> in various juices and H<sub>2</sub>O<sub>2</sub> disinfectant with Fe<sup>3+</sup>/CQDs or Fe<sup>2+</sup>/CQDs gave the recoveries of 87.8%–117.5% and 99.2%–106.4% with relative standard deviations (RSD) of 1.6–5.1% and 1.7–3.1%, respectively, showing satisfactory results for the determination of AA and H<sub>2</sub>O<sub>2</sub> in actual application. The proposed strategy may provide a new pathway to developing inexpensive and sensitive way for the detection of various redox reaction-involved system.

**Keywords** Carbon quantum dots · Nitrogen and sulfur co-doping · Fluorescent probe · Ascorbic acid · Hydrogen peroxide

## Introduction

Ascorbic acid (AA), or vitamin C (VC), is a common water-soluble vitamin with good antioxidant properties. It plays a key role in human metabolism and growth [1]. However, the AA can't be synthesized or converted by the body itself [2], and its lack can lead to scurvy, colds, mental disease and infertility [3–5]. Meanwhile, AA can promote the synthesis of collagen, enhancing the body resistance [6]. The daily needs of the human body for VC are mainly obtained by ingesting fruit. The change of the VC content is one of the important

indicators to judge the freshness and storage of fruits. In this regard, it is of great significance to establish a rapid and effective method for detecting the VC in fruits. Many methods for AA detection, including electrochemistry [7, 8], high performance liquid chromatography (HPLC) [9, 10], colorimetric [11] and etc. Although these methods can meet the requirement of sensitivity, they are usually time-consuming, cumbersome, expensive or the need of complex synthesis or complicated extraction process. The fluorescent assay technique received extensive attention because of the advantages of high sensitivity, good reproducibility, easy to realize real-time, and in situ monitoring [12–14].

Hydrogen peroxide (H<sub>2</sub>O<sub>2</sub>) is a relatively common peroxide, which is often used as an oxidant, bleach agent and disinfectant in real life. H<sub>2</sub>O<sub>2</sub> plays an important role in biological metabolism and environmental engineering. However, under normal circumstances, H<sub>2</sub>O<sub>2</sub> is easily decomposed into water and oxygen, not easy to exist for a long time. On October 27, 2017, the World Health Organization's International Agency for Research on Cancer published a preliminary list of carcinogens, H<sub>2</sub>O<sub>2</sub> is in the list of three types of

**Electronic supplementary material** The online version of this article (<https://doi.org/10.1007/s10895-019-02395-z>) contains supplementary material, which is available to authorized users.

✉ Xinyu Jiang  
jiangxinyu@csu.edu.cn

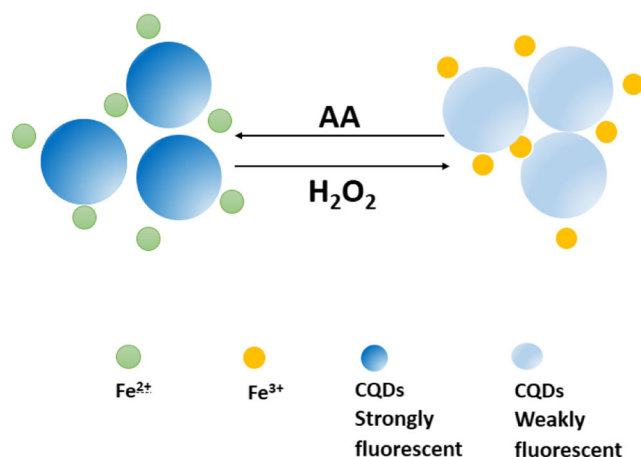
<sup>1</sup> School of Chemistry and Chemical Engineering, Central South University, Changsha 410083, China

<sup>2</sup> Key Laboratory of Hunan Province for Water Environment and Agriculture Product Safety, Changsha 410083, China

carcinogens. Therefore, it is of great significance to develop a rapid and accurate detection method for  $\text{H}_2\text{O}_2$ .

Over the last decade, carbon quantum dots (CQDs) have got extensive attention because of its unique properties, including tunable photoluminescence, molecular size, excellent photostability, low toxicity, chemical inertness, good solubility, biocompatibility, and ease of functionalization [15–17]. Lately, a large mass of fluorescent probes have been developed to the monitoring of metal ions [18–20]. For example, green fluorescent nitrogen-rich quantum dots (N-dots) served as a turn-off chemosensor for rapid and selective detection of  $\text{Hg}^{2+}$  and  $\text{Ag}^+$  in aqueous solutions [21]. A reusable P, N-doped carbon quantum dot was utilized as an efficient probe for detecting cobalt ion [22].

In this paper, an inexpensive way to synthesize multifunctional S,N-CQDs by utilizing citric acid (CA) and methionine (Met) was developed. Interestingly, the luminescence intensity of S,N-CQDs was effectively quenched by  $\text{Fe}^{3+}$ . Meanwhile, as we all know, the  $\text{Fe}^{3+}$  could be converted into  $\text{Fe}^{2+}$  under the presence of ascorbic acid or  $\text{Fe}^{2+}$  could be converted to  $\text{Fe}^{3+}$  under  $\text{H}_2\text{O}_2$ . Accordingly, on the basis of the fluorescence quenching mechanism and the principle of chemical reaction, we proposed an experimental strategy for rapid monitoring of AA and  $\text{H}_2\text{O}_2$ . The proposed method is depicted in Scheme 1. Initially, the luminescence of S,N-CQDs could be quenched by the iron(III). However, when AA is added to the system, iron(III) ions are reduced to iron(II) ions, the recovery efficiency of luminescence intensity displayed a linear fluorescent response to the concentration of AA. Finally, the iron(II) ions could be oxidized to iron(III) ions under the presence of  $\text{H}_2\text{O}_2$ . The fluorescence intensity will be annihilated again due to the iron(III) ions.



**Scheme 1** Design and principle for AA and  $\text{H}_2\text{O}_2$  detection use S,N-CQDs/ $\text{Fe}^{3+}$  or S,N-CQDs/ $\text{Fe}^{2+}$  system.

## Experimental Section

### Materials and Reagents

Citric acid,  $\text{FeCl}_3 \cdot 6\text{H}_2\text{O}$ ,  $\text{FeCl}_2 \cdot 4\text{H}_2\text{O}$ , trimethylaminomethane, NaOH, HCl, KCl, NaCl,  $\text{NH}_4\text{Cl}$ ,  $\text{Na}_2\text{SO}_4$ ,  $\text{Al}(\text{NO}_3)_3$ ,  $\text{NaH}_2\text{PO}_4$ ,  $\text{Na}_2\text{HPO}_4$ ,  $\text{Zn}(\text{NO}_3)_2$ ,  $\text{CaCl}_2$ ,  $\text{MgSO}_4$ ,  $\text{MnCl}_2$ ,  $\text{H}_2\text{O}_2$ ,  $\text{Ni}(\text{NO}_3)_2$ ,  $\text{CuSO}_4$ ,  $\text{Cd}(\text{NO}_3)_2$ ,  $\text{Pb}(\text{NO}_3)_2$ , glucose, were purchased from Sinopharm Chemical Reagent Co., Ltd. (Shanghai, China). Quinine sulfate, ascorbic acid, N-2-Hydroxyethylpiperazine-*N'*-2-ethylsulfonyl (HEPES), Amino acids (Cys, Try, His, Tyr, Trp, Phe, Met) were purchased from Aladdin (Shanghai, China). All reagents were analytical reagent grade. Water used in the experiment ( $18.2 \text{ M}\Omega \text{ cm}$ ) was purified by a Millipore-Q system.

### Apparatus

The size and morphology of S,N-CQDs was characterized by performing on an electronic microscope (TEM, Hitachi). Fourier transform infrared spectroscopy (FT-IR) was recorded by a Bruker IFS 66v/S infrared spectrophotometer (Bruker Optics Inc., Billerica, MA, USA). The crystalline phases of S,N-CQDs were characterized using a Rigaku D/max 2550 X-ray diffractometer (XRD). All absorption spectra were measured on a UV-2600 UV-Vis spectrophotometer (Shimadzu, Japan). The chemical composition and state of S,N-CQDs were investigated by PHI Quantera II X-ray photoelectron spectroscopy (XPS, Thermo Fisher Scientific 250Xi). Fluorescence spectra were measured on a LS-55 spectrofluorometer with excitation slit width of 10 nm and emission slit width of 15 nm (PerkinElmer, USA). The fluorescence lifetime was measured with Fluo Time 100 (PicoQuant, Germany). All pH measurements were made with a PHS-3E pH meter (Inesa Instrument, China).

### Preparation of S,N-CQDs

S,N-CQDs were synthesized via a one-step hydrothermal method. The detailed procedures are as follows: citric acid (4.5 g) and methionine (2 g) were mixed with ultrapure water (10.0 mL). And the mixture was then sonicated for 3 min to give a transparent solution. The solution was then transferred to a poly(tetrafluoroethylene) (Teflon)-lined autoclave (25 mL), heated at  $180 \text{ }^\circ\text{C}$  for 10 h and then cooled down to room temperature. The brown-yellow product was further purified by filtration ( $0.22 \text{ }\mu\text{m}$  nitrocellulose filters). After evaporating the solvent and further drying under vacuum, the S,N-CQDs were dispersed in the

aqueous solution as stock solution for later characterization and use.

### Detection of Fe<sup>3+</sup> Based on S,N-CQDs

In a typical assay of Fe<sup>3+</sup>, 20  $\mu$ L (50  $\mu$ g/mL) of S,N-CQDs was added to 280  $\mu$ L 50 mM Tris buffer solution which contained various of chemical species (Fe<sup>3+</sup>, Cu<sup>2+</sup>, Pb<sup>2+</sup>, Fe<sup>2+</sup>, K<sup>+</sup>, Zn<sup>2+</sup>, Cd<sup>2+</sup>, Mg<sup>2+</sup>, Al<sup>3+</sup>, Na<sup>+</sup>, Mn<sup>2+</sup>, Ni<sup>2+</sup>, NH<sub>4</sub><sup>+</sup>, Ca<sup>2+</sup>, Cys, Try, Phe, His, Tyr, Trp, glucose, AA, H<sub>2</sub>O<sub>2</sub>). Then, the fluorescence spectra were recorded after 1 min. In order to investigate the relationship between the different Fe<sup>3+</sup> concentrations and the fluorescence data of S,N-CQDs, different concentrations of a Fe<sup>3+</sup> solution were added to the system. The fluorescence spectra were measured with excitation at 330 nm (excitation bandwidth 10 nm).

### AA Sensing Based on S,N-CQDs/Fe<sup>3+</sup>

AA detection was realized as follows: different concentrations of AA were added to 300  $\mu$ L S,N-CQDs/Fe<sup>3+</sup> system (50  $\mu$ g/mL in 50 mM Tris-HCl, pH 6.0). Following that, the mixtures were transferred into a 400  $\mu$ L quartz cuvette. The fluorescence spectra of the final mixture solution were measured. (excited at 330 nm).

### Monitoring of H<sub>2</sub>O<sub>2</sub> Based on S,N-CQDs/Fe<sup>2+</sup>

For the H<sub>2</sub>O<sub>2</sub> detection, the H<sub>2</sub>O<sub>2</sub> solutions with varied concentrations were added to 300  $\mu$ L S,N-CQDs/Fe<sup>2+</sup> system (50  $\mu$ g/mL in 50 mM Tris-HCl, pH 6.0). Afterward, the mixtures were transferred into a 400  $\mu$ L quartz cuvette. The luminescence emission signals were measured with excitation at 330 nm.

### Real Sample Assay

A variety of fruits were purchased from the fruit shop (The orange, grapefruit and lemon are all fresh, Bubugao supermarket, Changsha, Hunan) and then fruit juices were squeezed out. Furthermore, to remove the matrix effect, real fruit juices filtered with a 0.45  $\mu$ m filter membrane was obtained and then diluted 10 times with ultrapure water. Vitamin C lozenge (The mass of the whole chewable tablet is 1 g and each tablet contains 0.1 g of vitamin C, Jiangxi Xinyijiang Pharmaceutical Co., Ltd.) was ground into powder with a mortar. After being diluted into an appropriate concentration with ultrapure water, AA with different concentrations was spiked into the real samples, which was detected following the as-provided strategy.

Medical hydrogen peroxide disinfectant (hydrogen peroxide 3%~3.5%, Yiyang Medical Research Institute,

Hunan Province) was purchased from a local clinic. The sample was diluted into an appropriate concentration with ultrapure water. Standard H<sub>2</sub>O<sub>2</sub> solution with different concentrations was spiked into the real samples, the fluorescence spectra were recorded at 395 nm (excited at 330 nm).

## Results and Discussion

### Characterization of S,N-CQDs

In order to study the structure and morphology of the prepared S,N-CQDs, a series of characterizations including TEM, FT-IR, XRD, UV-vis and XPS were conducted. As shown in Fig. 1a, uniform particle size distribution for S,N-CQDs can be observed and the S,N-CQDs are spherical and well-dispersed. As shown in Fig. 1b, FT-IR spectrum of S,N-CQDs reveals a band around 3404 cm<sup>-1</sup> correlated with OH stretching vibrations. Meanwhile, the peak at 2924 cm<sup>-1</sup> corresponds to the stretching of C-H. The peak at 1713 cm<sup>-1</sup> is attributed to C=O stretching vibration. The peak at 1654 cm<sup>-1</sup> might be attributed to C=C, C=O and C=N stretching in the conjugated structure [23]. The characteristic absorption bands of C-S-C stretching vibration at 1202 cm<sup>-1</sup> demonstrated the presence of S elements on the surface of S,N-CQDs. XRD results (Fig. 1c) showed that a broader peak around 23.5°, which indicated that the N,S-CQDs appeared to be amorphous carbon particles in nature [24, 25]. In UV-vis spectrum (Fig. 1d), there are two distinct absorption peaks. One can be assigned to n- $\sigma^*$  transition at 213 nm, which indicates the presence of -NH<sub>2</sub>. The other one might attribute to n- $\pi^*$  transition of C=O bond at 313 nm [26, 27].

The results of XPS analysis are shown in Fig. 2. Four distinct peaks around 164.0 eV, 286.0 eV, 399.0 eV, and 532.0 eV in Fig. 2a could be ascribed to sulfur, carbon, nitrogen and oxygen, respectively [28]. As shown in Fig. 2b, C1s spectrum could be divided into five main peaks corresponding to C=C, C-C (284.6 eV), C-S (285.2 eV), C-N (286.1 eV), C-O (286.8 eV), and C=N, C=O (288.4 eV) functional groups [29, 30] respectively. Deconvolution of N1 s spectra in Fig. 2c reveals two nitrogen species of -NH (399.6 eV) and C-N-C (400.0 eV) [31, 32]. The detailed information of sulfur could be characterized by the deconvoluted high resolution S2p spectrum in Fig. 2d. The peak at lower binding energy consisted of two peaks, in which peak at 163.3 eV and 164.6 eV was assigned to S2p<sub>3/2</sub> and S2p<sub>1/2</sub>, respectively [33].

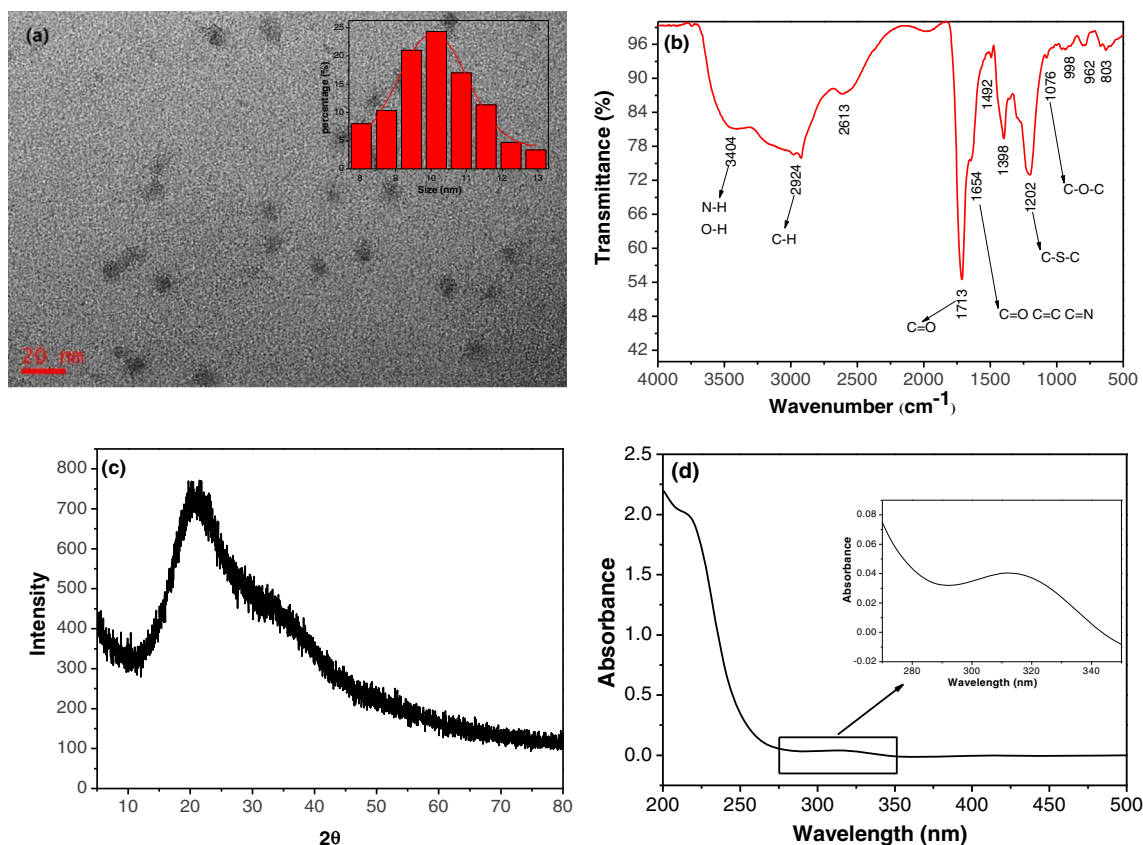


**Fig. 1** a TEM images of S, N-CQDs. (b) FT-IR spectra of S,N-CQDs. (c) XRD pattern of the S,N-CQDs. (d) UV-vis absorption spectrum of S,N-CQDs

### Fe<sup>3+</sup> Detection Performance

To test the specificity of this fluorescence probe, the fluorescence responses of S,N-CQDs upon addition of the potential interfering species were examined. Figure 3a displays the selectivity results of the method toward Fe<sup>3+</sup> in the presence of other interfering species. A dramatic fluorescence quenching was observed when Fe<sup>3+</sup> was added to the solution of S,N-CQDs, while no significant fluorescence decrease happened at the introduction of any other species, suggesting that this fluorescence system cannot be interfered by other species. The possible mechanism is that the introduced sulfur atoms seem to be able to eliminate the O-states and enhance the N-states, leading to that the original surface states nearly neglected in the N,S-CQDs.

Then the response of the S,N-CQDs at different Fe<sup>3+</sup> concentrations was evaluated. The fluorescence was gradually quenched with increasing concentration of Fe<sup>3+</sup> from 50 μM to 1000 μM (Fig. 3b). Additionally, Fig. 3c and Fig. 3d displays the fluorescence data versus the different Fe<sup>3+</sup> concentrations. The fluorescence intensity at 395 nm was linearly correlated with the Fe<sup>3+</sup> concentration in the range of 50–300 μM ( $R^2 = 0.995$ ) and 300–800 μM ( $R^2 = 0.981$ ), respectively. The

detection limit (in terms of the 3σ rule) was calculated to be 5.0 μM.

### AA Sensing Performance

To further explore the selectivity of this nanosystem for AA, other potential interferents including a variety of metal ions, amino acids, and organics (AA, Fe<sup>2+</sup>, K<sup>+</sup>, Mg<sup>2+</sup>, Na<sup>+</sup>, Ca<sup>2+</sup>, Cys, Try, Phe, His, glucose) were incubated with a mixed solution of S,N-CQDs/Fe<sup>3+</sup>. Figure 4a vividly shows the fluorescence recovery degree under different species. Obviously, the mixture solution of AA and S,N-CQDs/Fe<sup>3+</sup> exhibited the highest fluorescence recovery relative to other interferents, revealing that the N,S-CQDs/Fe<sup>3+</sup> composite possessed high specificity toward AA under the presence of other interfering species. In addition, the fluorescence intensity of S,N-CQDs/Fe<sup>3+</sup> at around 395 nm increased gradually with increasing AA concentrations (Fig. 4b). Figure 4c depicts the feasibility that S,N-CQDs/Fe<sup>3+</sup> as excellent probe in the detection of AA. As indicated in Fig. 4d, the enhancement of FL had a good linearity to the AA concentration in the range from 50 to 500 μM and the limit of detection (LOD) was 4.2 μM. As shown in Fig. S1, AA performed different fluorescence recovery effect in different buffer solutions.

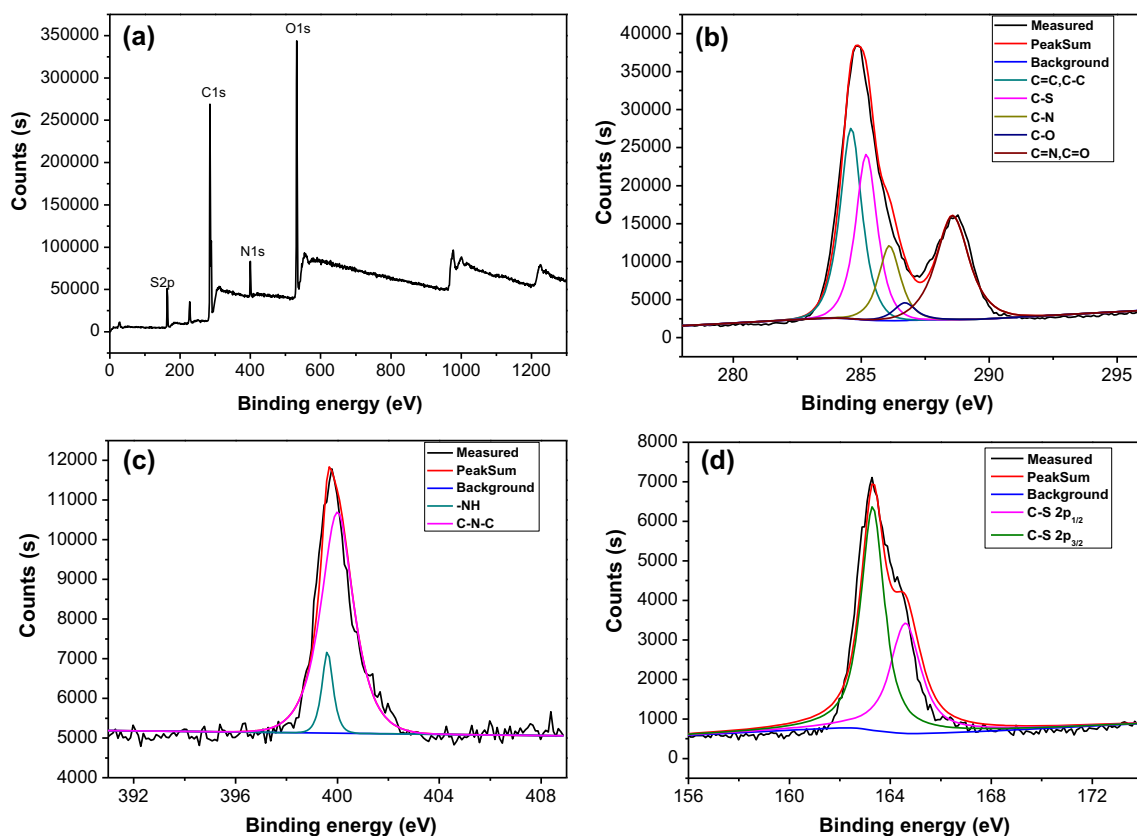
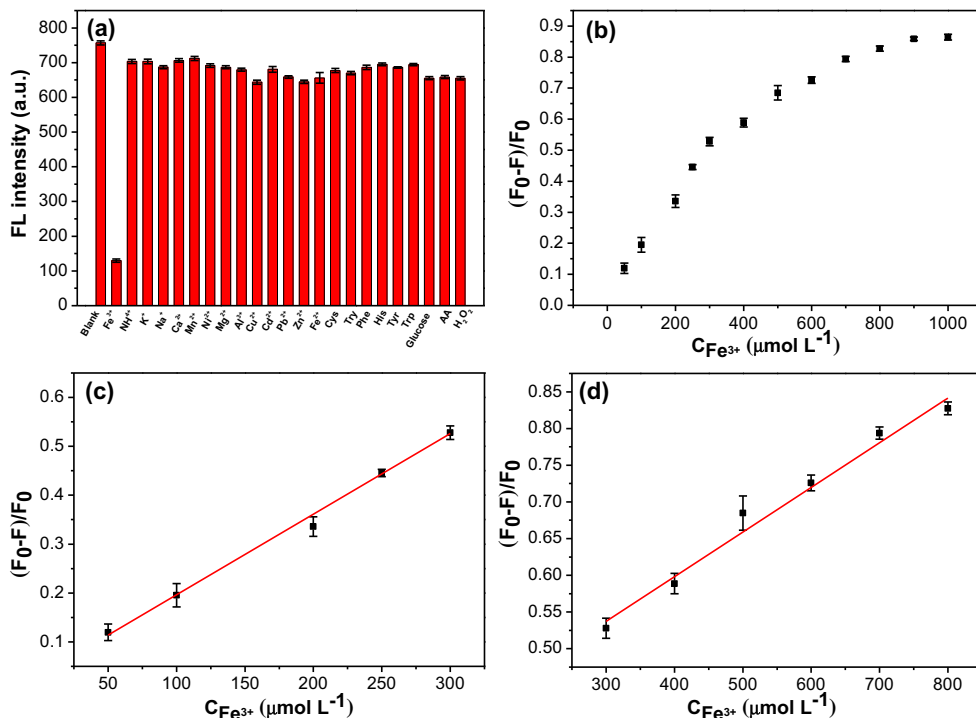


**Fig. 2** **a** XPS spectrum of S,N-CQDs. **b** High-resolution XPS spectra of C1s, **c** N1 s and **(d)** S2p

But only in Tris-HCl buffer, AA had the best fluorescence recovery effect. The pH stability of S,N-CQDs/Fe<sup>3+</sup>

system is displayed in Fig. S 2a, in which fluorescence intensity changed little in the pH range from 3 to 12.

**Fig. 3** **a** Selectivity of 50 μg/mL N, S-CQDs after adding different metal ions and other interferences with the same concentration of 1 mM. **b** The relationships between  $(F_0 - F)/F_0$  and Fe<sup>3+</sup> ions (50–1000 μM). **c** The relationship between  $(F_0 - F)/F_0$  and Fe<sup>3+</sup> from 50 to 300 μM. **(d)** The relationship between  $(F_0 - F)/F_0$  and Fe<sup>3+</sup> from 300 to 800 μM.  $F$  and  $F_0$  are the FL intensities of S,N-CQDs in the presence and absence of Fe<sup>3+</sup>, respectively. All data represent the fluorescence intensity at 395 nm in the 50 mM Tris-HCl buffer at pH 6.0,  $\lambda_{exc} = 330$  nm



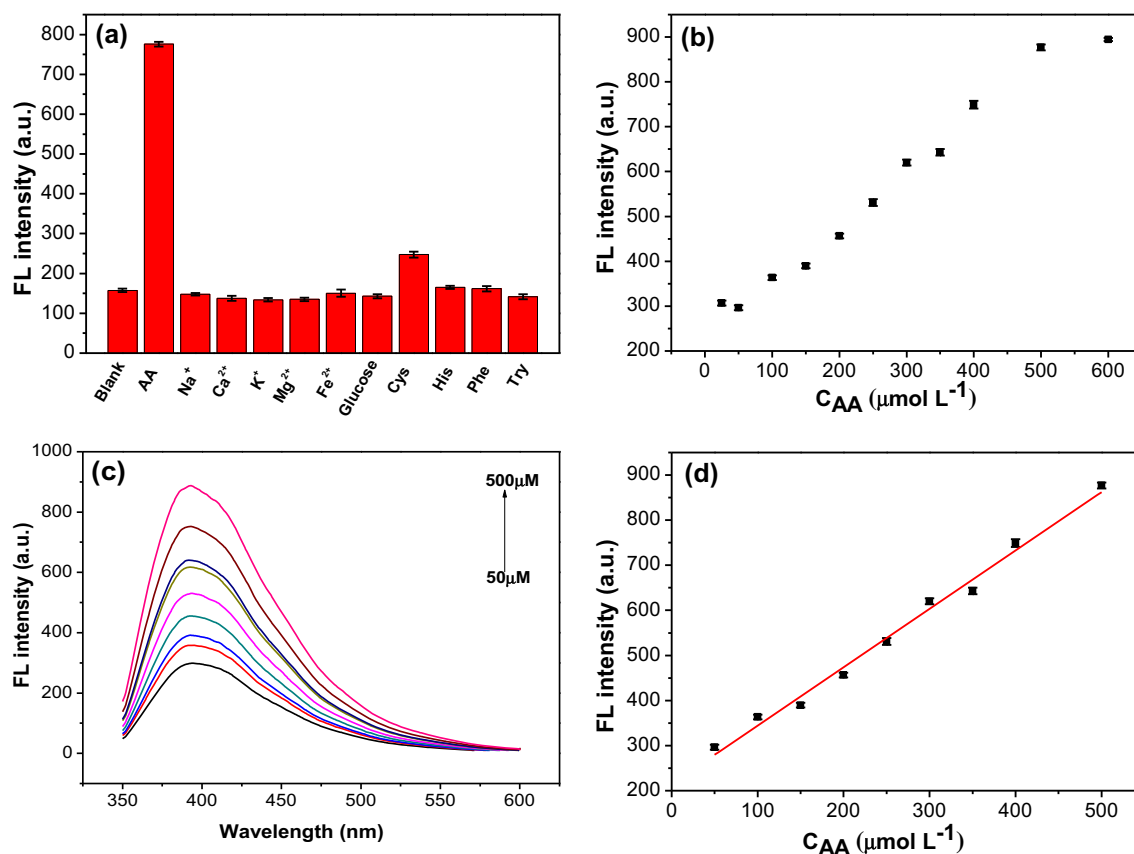


**Fig. 4** **a** FL responses of the S, N-CQDs/Fe<sup>3+</sup> system towards different chemicals at the concentration of 1 mM (the concentration of AA is 600 μM). **b** FL responses of the S, N-CQDs/Fe<sup>3+</sup> system towards different concentrations of AA (25, 50, 100, 150, 200, 250, 300, 350,

400, 500, 600 μM). **c** Representative fluorescence emission spectra of S, N-CQDs/Fe<sup>3+</sup> in the presence of increasing AA concentrations (50–500 μM) in 50 mM Tris-HCl buffer at pH 6.0. **d** Plot of FL responses of S, N-CQDs/Fe<sup>3+</sup> vs concentration of AA from 50 to 500 μM

## H<sub>2</sub>O<sub>2</sub> Monitoring Performance

The selectivity of S,N-CQDs/Fe<sup>2+</sup> toward H<sub>2</sub>O<sub>2</sub> was evaluated by screening its response to metal ions, amino acids and organics (H<sub>2</sub>O<sub>2</sub>, AA, K<sup>+</sup>, Mg<sup>2+</sup>, Na<sup>+</sup>, Ca<sup>2+</sup>, Cys, Try, Phe, His, glucose, Tyr). As indicated in Fig. 5a, the fluorescence intensity was the feeblest when H<sub>2</sub>O<sub>2</sub> was added to the S,N-CQDs/Fe<sup>2+</sup> system, suggesting that S,N-CQDs/Fe<sup>2+</sup> could be applied to selectively monitor H<sub>2</sub>O<sub>2</sub> in aqueous solution. In contrast, no obvious decrease in fluorescent intensity could be observed by adding other interfering species. For the sake of achieving good quenching effect, the appropriate Fe<sup>2+</sup> concentration was also optimized. As shown in Fig. 5b, when the Fe<sup>2+</sup> concentration reached 1 mM, the fluorescence intensity of S,N-CQDs could be well quenched. Under optimized condition, we explored the application of S,N-CQDs/Fe<sup>2+</sup> as a fluorescence sensing for the measurement of H<sub>2</sub>O<sub>2</sub>. Figure 5c depicts the fluorescence spectroscopy recovery of S,N-CQDs/Fe<sup>2+</sup> composite system after adding different concentrations of H<sub>2</sub>O<sub>2</sub>, implying the feasibility that S,N-CQDs/Fe<sup>2+</sup> as excellent probe in the detection of H<sub>2</sub>O<sub>2</sub>. Figure 5d illustrates the relationship between the fluorescence intensity at 395 nm with

various concentrations of H<sub>2</sub>O<sub>2</sub>. A linear calibration in the scope of 10 to 140 μM ( $R^2 = 0.996$ ) was constructed. The detection limit of H<sub>2</sub>O<sub>2</sub> was calculated to be 1.9 μM according to the equation  $3\sigma/S$ . Moreover, as shown in Fig. S 2b, the effect of pH was also investigated, the result shows fluorescence intensity of S,N-CQDs/Fe<sup>2+</sup> dropped sharply in the case of alkaline condition.

## Application in Real Samples

Practical application for the development of S,N-CQDs/Fe<sup>3+</sup> and S,N-CQDs/Fe<sup>2+</sup> as fluorescent probes was exploited. For the purpose of verifying the method, standard addition experiments were carried out with fruit juices and hydrogen peroxide disinfectant. Table 1 shows the AA test results, the relative standard deviation (RSD) was lower than 5.1 and the recoveries were found to be varied between 87.8% and 117.5% for the samples of various fruit juices. Table 2 shows the H<sub>2</sub>O<sub>2</sub> test results, RSD was found to be lower than 3.1 with the recoveries between 99.2% and 106.4% for the detection of hydrogen peroxide disinfectant.

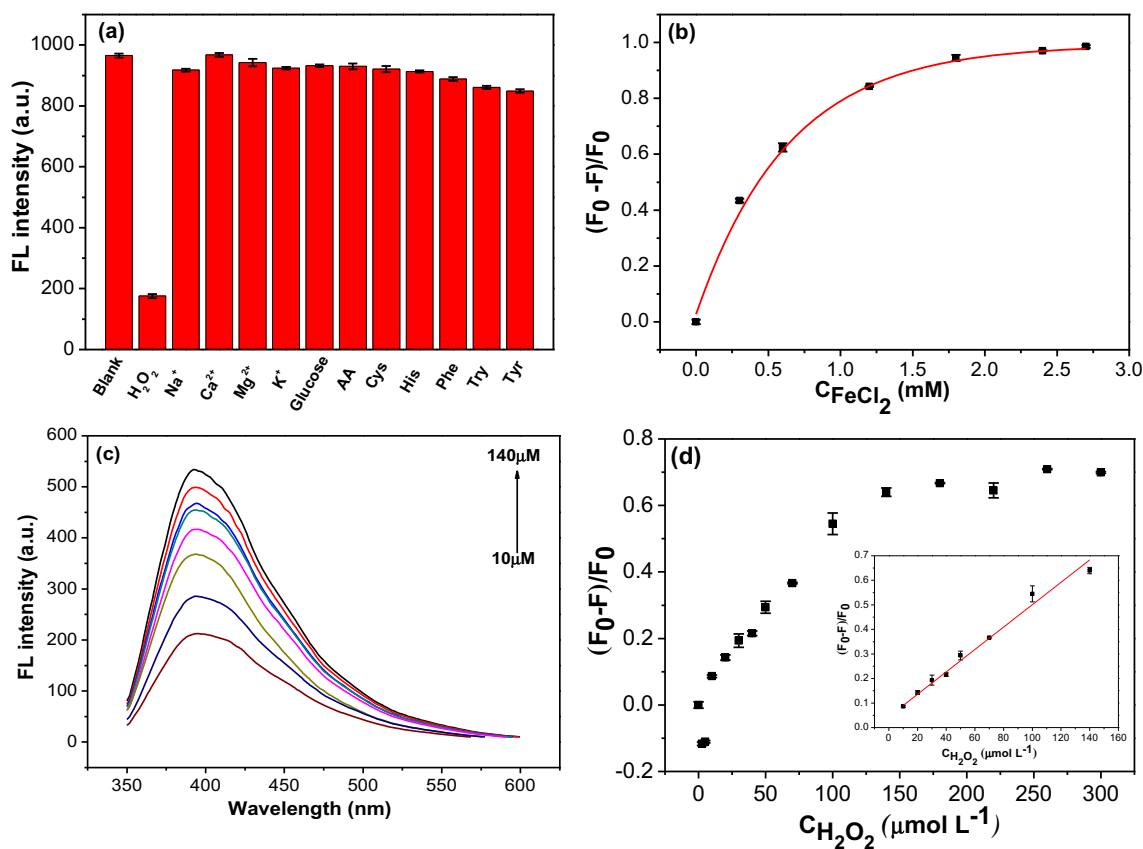


**Fig. 5** **a** FL responses of the S, N-CQDs/Fe<sup>2+</sup> system towards different chemicals at the concentration of 1 mM (the concentration of H<sub>2</sub>O<sub>2</sub> is 300 μM). **b** The relationships between (F<sub>0</sub>-F)/F<sub>0</sub> and Fe<sup>2+</sup> (0.3–2.7 μM) in the presence of 500 μM H<sub>2</sub>O<sub>2</sub>. **c** Representative fluorescence emission

spectra of S, N-CQDs/Fe<sup>2+</sup> in the presence of increasing H<sub>2</sub>O<sub>2</sub> concentrations in 50 mM Tris-HCl buffer at pH 6.0. **(d)** The relationships between (F<sub>0</sub>-F)/F<sub>0</sub> and H<sub>2</sub>O<sub>2</sub> (2.5–300 μM)

**Table 1** AA detection in diverse real samples

| Sample           | Added (μM) | Found <sup>a</sup> (μM) | Recovery (%) | RSD (%)<br>n = 3 |
|------------------|------------|-------------------------|--------------|------------------|
| Vitamin C        | 0          | 186.4                   | –            | 2.8              |
|                  | 50.0       | 286.5                   | 114.6        | 3.5              |
|                  | 100.0      | 318.4                   | 106.1        | 4.1              |
| Orange juice     | 200.0      | 357.2                   | 89.3         | 2.3              |
|                  | 0          | 244.3                   | –            | 2.4              |
|                  | 50.0       | 258.4                   | 87.8         | 3.4              |
|                  | 100.0      | 337.4                   | 94.1         | 1.6              |
| Grapefruit juice | 200.0      | 475.2                   | 106.9        | 4.8              |
|                  | 0          | 107.9                   | –            | 5.1              |
|                  | 50.0       | 174.5                   | 110.5        | 3.7              |
|                  | 100.0      | 198.7                   | 95.6         | 1.9              |
| Lemon juice      | 200.0      | 301.9                   | 98.0         | 4.6              |
|                  | 0          | 140.7                   | –            | 4.5              |
|                  | 50.0       | 174.6                   | 91.6         | 2.7              |
|                  | 100.0      | 282.8                   | 117.5        | 3.8              |
|                  | 200.0      | 371.7                   | 109.1        | 1.9              |

<sup>a</sup> Average of three measurements

### Conclusions

In conclusion, the synthetic S,N-CQDs were thoroughly characterized by chemical morphology and structural analysis, affirming the presence of various functional groups associated with sulfur and nitrogen. Moreover, the fluorescence intensity of S,N-CQDs was effectively quenched by Fe<sup>3+</sup> and then facily recovered with the addition of AA. On the basis of the fluorescence quenching-recovery principle, we proposed an experimental strategy for the determination of strongly reducing and oxidizing substances based on a simple redox

**Table 2** H<sub>2</sub>O<sub>2</sub> detection in real sample

| Sample                         | Added (μM) | Found <sup>a</sup> (μM) | Recovery (%) | RSD (%)<br>n = 3 |
|--------------------------------|------------|-------------------------|--------------|------------------|
| Hydrogen peroxide disinfectant | 0          | 34.5                    | –            | 1.7              |
|                                | 30.0       | 62.7                    | 104.5        | 2.5              |
|                                | 60.0       | 89.3                    | 99.2         | 3.1              |
|                                | 90.0       | 127.2                   | 106.4        | 2.2              |

<sup>a</sup> Average of three measurements

principle and the proposed method has been successfully applied to selective monitoring of AA and  $H_2O_2$  in an enzyme-free and label-free way. The as prepared S,N-CQDs/ $Fe^{3+}$  and S,N-CQDs/ $Fe^{2+}$  might provide an effective way for the measuring of various redox reaction-involved system, and might have great potential for food industry monitoring and commercial testing.

**Acknowledgements** We gratefully acknowledge the National Natural Science Foundation of China (No. 21571191 and No. 51674292) and Key Laboratory of Hunan Province for Water Environment and Agriculture Product Safety (2018TP1003).

## References

- Jing-Jing Liu Z-TC, Tang D-S, Wang Y-B, Long-Tian Kang J-NY (2015) Graphene quantum dots-based fluorescent probe for turn-on sensing of ascorbic acid. *Sensors Actuators B Chem* 212:214–219
- Meng H, Yang D, Tu Y, Yan J (2017) Turn-on fluorescence detection of ascorbic acid with gold nanoclusters. *Talanta* 165:346–350
- Frajese GV, Benvenuto M, Fantini M, Ambrosin E, Sacchetti P, Masuelli L, Giganti MG, Modesti A, Bei R (2016) Potassium increases the antitumor effects of ascorbic acid in breast cancer cell lines in vitro. *Oncol Lett* 11(6):4224–4234
- Pournaghi-Azar MH, Razmi-Nerbin H, Hafezi B (2001) Amperometric determination of ascorbic acid in real samples using an aluminum electrode, modified with nickel Hexacyanoferrate films by simple Electroless dipping method. *Electroanal* 14(3):206–212
- Ntei Abudu JJM, Attaelmannan M, Levinson SS (2004) Vitamins in human arteriosclerosis with emphasis on vitamin C and vitamin E. *Clin Chim Acta* 339:11–25
- May JM, Qu ZC (2005) Transport and intracellular accumulation of vitamin C in endothelial cells: relevance to collagen synthesis. *Arch Biochem Biophys* 434(1):178–186
- Xiaomin QIANQZ, Ying ZHANG aYT (2010) Separation/determination of flavonoids and ascorbic acid in rat serum and excrement by capillary electrophoresis with electrochemical detection. *Anal Sci* 26(5):557–560
- Khairy M, Mahmoud BG (2016) Copper oxide microstructures with hemisphere pineapple morphology for SelectiveAmperometric determination of vitamin C(L-ascorbic acid) in human fluids. *Electroanal* 28(10):2606–2612
- Lima DRS, Cossenza M, Garcia CG, Portugal CC, Marques FFC, Paes-de-Carvalho R, Pereira Netto AD (2016) Determination of ascorbic acid in the retina during chicken embryo development using high performance liquid chromatography and UV detection. *Anal Methods* 8:5441–5447
- Matsuoka Y, Yamato M, Yamasaki T, Mito F, Yamada K (2012) Rapid and convenient detection of ascorbic acid using a fluorescent nitroxide switch. *Free Radical Bio Med* 53(11):2112–2118
- Danyang Ji YD, Meng H, Lin Z, Huang Z, Hu Y, Jianjun Li FY, Li Z (2018) A novel colorimetric strategy for sensitive and rapid sensing of ascorbic acid using cobalt oxyhydroxide nanoflakes and 3,3', 5,5'-tetramethylbenzidine. *Sensors Actuators B Chem* 256:512–519
- Nuo Duan SW, Dai S, Miao T, Jie Chen ZW (2015) Simultaneous detection of pathogenic bacteria using an aptamer based biosensor and dual fluorescence resonance energy transfer from quantum dots to carbon nanoparticles. *Microchim Acta* 182:917–923
- Matsuoka Y, Yamato M, Yamada K (2016) Fluorescence probe for the convenient and sensitive detection of ascorbic acid. *J Clin Biochem Nutr* 58:16–22
- Feng LL, Wu YX, Zhang DL, Hu XX, Zhang J, Wang P, Song ZL, Zhang XB, Tan W (2017) Near infrared graphene quantum dots-based two-photon Nanoprobe for direct bioimaging of endogenous ascorbic acid in living cells. *Anal Chem* 89(7):4077–4084
- Tran Van Tam NBT, Kim HR, Chung JS, Choi WM (2014) One-pot synthesis of N-doped graphene quantum dots as a fluorescent sensing platform for  $Fe^{3+}$  ions detection. *Sensors Actuators B Chem* 202:568–573
- IGA PMC a, Yate b L, Zaera RT, Cabanero G, Grande HJ, Ruiz V (2016) Graphene quantum dot membranes as fluorescent sensing platforms for Cr (VI) detection. *Carbon* 109:658–665
- Li N, Than A, Wang X, Xu S, Sun L, Duan H, Xu C, Chen P (2016) Ultrasensitive profiling of metabolites using tyramine-functionalized graphene quantum dots. *ACS Nano* 10(3):3622–3629
- Weng CI, Chang HT, Lin CH, Shen YW, Unnikrishnan B, Li YJ, Huang CC (2015) One-step synthesis of biofunctional carbon quantum dots for bacterial labeling. *Biosens Bioelectron* 68:1–6
- He J, Zhang H, Zou J, Liu Y, Zhuang J, Xiao Y, Lei B (2016) Carbon dots-based fluorescent probe for "off-on" sensing of hg(II) and I. *Biosens Bioelectron* 79:531–535
- Gong X, Liu Y, Yang Z, Shuang S, Zhang Z, Dong C (2017) An "on-off-on" fluorescent nanoprobe for recognition of chromium(VI) and ascorbic acid based on phosphorus/nitrogen dual-doped carbon quantum dot. *Analy Chim Acta* 968:85–96
- Zhisheng Wu MF, Chen X, Tang X (2016) N-dots as a photoluminescent probe for the rapid and selective detection of  $Hg^{2+}$  and  $ag^+$  in aqueous solution. *J Mater Chem B* 4:2086
- Sen Liao FZ, Zhao X, Yang H, Chen X (2018) A reusable P, N-doped carbon quantum dot fluorescent sensor for cobalt ion. *Sensors Actuators B Chem* 260:156–164
- Siriwardana K, Nettles CB 2nd, Vithanage BC, Zhou Y, Zou S, Zhang D (2016) On-resonance fluorescence, resonance Rayleigh scattering, and Ratiometric resonance synchronous spectroscopy of molecular- and quantum dot-fluorophores. *Anal Chem* 88(18):9199–9206
- Tang L, Ji R, Cao X, Lin J, Jiang H, Li X, Teng KS, Luk CM, Zeng S, Hao J, Lau SP (2012) Deep ultraviolet photoluminescence of water-soluble self-passivated graphene quantum dots. *ACS Nano* 6:5102–5110
- Liu R, Wu D, Feng X, Mullen K (2011) Bottom-up fabrication of photoluminescent graphene quantum dots with uniform morphology. *J Am Chem Soc* 133(39):15221–15223
- Mehta VN, Jha S, Basu H, Singhal RK, Kailasa SK (2015) One-step hydrothermal approach to fabricate carbon dots from apple juice for imaging of mycobacterium and fungal cells. *Sensors Actuators B Chem* 213:434–443
- Jiang K, Zhang L, Lu J, Xu C, Cai C, Lin H (2016) Triple-mode emission of carbon dots: applications for advanced anti-counterfeiting. *Angew Chem* 55(25):7231–7235
- Dong Sun RB, Zhang P-H, Wu G-H, Zhang J-R, Zhu J-J (2013) Hair fiber as a precursor for synthesizing of sulfur- and nitrogen-co-doped carbon dots with tunable luminescence properties. *Sci Direct* 64:424–434
- DSa W-JN, Zhu R-H, Deng S-Y, Cosnier S, Zhang X-J (2016) Dumbbell-shaped carbon quantum dots/AuNCs nanohybrid as an



- efficient ratiometric fluorescent probe for sensing cadmium (II) ions and L-ascorbic acid. *Carbon* 96:1034–1042
30. Zhongqian Song FQ, Xu Y, Liu M, Cui L, Liu J (2016) Multifunctional N,S co-doped carbon quantum dots with pH- and thermo-dependent switchable fluorescent properties and highly selective detection of glutathione. *Carbon* 104:169–178
  31. Jiang K, Sun S, Zhang L, Wang Y, Cai C, Lin H (2015) Bright-yellow-emissive N-doped carbon dots: preparation, cellular imaging, and bifunctional sensing. *ACS Appl Mater Inter* 7(41):23231–23238
  32. Hou J, Wang W, Zhou T, Wang B, Li H, Ding L (2016) Synthesis and formation mechanistic investigation of nitrogen-doped carbon dots with high quantum yields and yellowish-green fluorescence. *Nanoscale* 8(21):11185–11193
  33. Wei Li MZ, Li H, Wang K, Cheng S, Jiang K (2015) A high performance sulfur-doped disordered carbon anode for sodium ion batteries. *Energ Environ Sci* 8:2916

**Publisher's Note** Springer Nature remains neutral with regard to jurisdictional claims in published maps and institutional affiliations.